Mechanism of Chaperone-like Activity. Suppression of Thermal Aggregation of β_L-Crystallin by α-Crystallin[†]

Helen A. Khanova,[‡] Kira A. Markossian,[‡] Boris I. Kurganov,*[,‡] Alexander M. Samoilov,[‡] Sergey Yu. Kleimenov,[‡] Dmitrii I. Levitsky,[‡] Igor K. Yudin,[§] Antonina C. Timofeeva,[∥] Konstantin O. Muranov,[⊥] and Michail A. Ostrovsky[⊥]

Bach Institute of Biochemistry, Russian Academy of Sciences, Leninsky 33, 119071, Moscow, Russia, School of Biology of Moscow State University, Vorobjevy gory 1, 119992, Moscow, Russia, Emanuel Institute of Biochemical Physics, Russian Academy of Sciences, Kosygina 4, 119991, Moscow, Russia, and Oil and Gas Research Institute, Russian Academy of Sciences, Gubkina St., 3, 117971, Moscow, Russia

Received June 18, 2005; Revised Manuscript Received September 27, 2005

ABSTRACT: Thermal denaturation and aggregation of β_L-crystallin from bovine lens have been studied using differential scanning calorimetry (DSC) and dynamic light scattering (DLS). According to the DLS data, the distribution of the β_L-crystallin aggregates by their hydrodynamic radius (R_h) remains monomodal to the point of precipitating aggregates (sodium phosphate, pH 6.8; 100 mM NaCl; 60 °C). The size of the start aggregates ($R_{h,0}$) and duration of the latent stage (t_0) leading to the formation of the start aggregates have been determined from the light scattering intensity versus the hydrodynamic radius plots and the dependences of R_h on time. The $R_{h,0}$ value remains constant at variation of the β_L-crystallin concentration, whereas the t_0 value increases with diminishing β_L-crystallin concentration. The suppression of β_L-crystallin aggregation by α-crystallin is connected with the decrease in the $R_{h,0}$ value and increase in the t_0 value. In the presence of α-crystallin the aggregate population is split into two components. The first component is represented by stable aggregates whose size remains constant in time. The aggregates of the other kind grow until they reach the size characteristic of aggregates prone to precipitation. The DSC data show that α-crystallin has no appreciable influence on thermal denaturation of β_L-crystallin.

In mammal eye lenses, there are three classes of crystallins denoted α, *β*, and *γ*. α-Crystallin, the major lens protein a member of a small heat shock protein family, acts as a molecular chaperone (*1*−*3*), whereas *β*- and *γ*-crystallins are structural proteins (*4*, *5*). Crystallins with monomeric molecular weights of approximately 20−30 kDa form high-molecular-weight aggregates. The stability and transparency of the lens depend on the proper assembly of these aggregates (*4*, *5*). In the lens, α-crystallin protects *β*- and *γ*-crystallins against nonspecific aggregation through its chaperone-like activity (*6*, *7*). Protection of *β*- and *γ*-crystallins against aggregation, which owes to the chaperone-like activity of α-crystallin, is of great importance, since no protein turnover occurs in the center of the lens (*8*). Loss of the chaperone-like activity of α-crystallin results from its posttranslational modifications, and may be accompanied by aggregation of *β*- and *γ*-crystallins and development of cataract (*5*, *9*, *10*).

α-Crystallin has been shown to inhibit aggregation of a wide range of proteins under in vitro stress conditions (elevated temperature, chemical reduction, or oxidation) (*1*, *11*−*17*). The mechanism of chaperoning of substrate proteins by α-crystallin is not well understood. It has been reported that the ability of α-crystallin to suppress heat-induced aggregation of proteins is a result of hydrophobic interactions with these denatured proteins, and that this ability increases when α-crystallin is heated (*11*, *18*). α-Crystallin undergoes a thermal transition at 60 °C. That results in partial unfolding of the protein, which then doubles in molecular weight and increases in size (*17*−*22*), but does not aggregate further (*23*). β_L-Crystallin also starts to unfold around 60 °C (*21*). It has been demonstrated that α-crystallin is able to associate with β_L-crystallin at the beginning of its thermal denaturation, thus preventing aggregation and precipitation, and no reaction occurs between α-crystallin and the completely heat-denatured protein (*1*, *11*, *24*). The increase of α-crystallin in size is accompanied by the changes in environments around tryptophan and cysteine residues (*21*). The hydrophobic tryptophan residues move to the surface of the protein and thereby increase external hydrophobic interactions (*25*). A high-temperature stress, inducing a partial unfolding of β_L-crystallin and structural transition in α-crystallin, results in the formation of a new dynamic structure. In this conformation, α-crystallin can form stable soluble complexes with denatured β_L-crystallin via multiple interactive surfaces over a wide range of protein concentrations (*21*). Increasing the concentration of α-crystallin has the same effect as heating (*25*). Thus, α-crystallin temperature-induced modifications were found necessary to allow for the association with denatured β_L-crystallin.

[†] This study was funded by the Russian Foundation for Basic Research (Grant 05-04-48691), Programs "Molecular and Cell Biology" and "Basic Sciences to Medicine" of the Presidium of the Russian Academy of Sciences, and by INTAS (Grant 03-51-4813).

* To whom correspondence should be addressed. Tel: (7-095) 952-5641. Fax: (7-095) 954-2732. E-mail: boris@kurganov.com.

[‡] Bach Institute of Biochemistry.

[§] Oil and Gas Research Institute.

[∥] Moscow State University.

[⊥] Emanuel Institute of Biochemical Physics.

10.1021/bi051175u CCC: $30.25
Published on Web 11/03/2005

It is of interest that α-crystallin has the ability to specifically inhibit nucleation-dependent aggregation of proteins (*26*). This ability has been demonstrated by selective suppression of aggregation of the serine proteinase inhibitors by α-crystallin at 50 °C. The nucleation-dependent aggregation of α_1-antichymotrypsin is suppressed by α-crystallin, whereas the nucleation-independent aggregation of α_1-antitrypsin is insensitive to α-crystallin.

The basic models of protein aggregation have been recently discussed by Speed et al. (*27*). These models include (1) sequential particle−cluster aggregation, in which monomeric units add individually to a growing aggregate; (2) multimeric cluster−cluster aggregation, in which multimers of any size associate, and no sequential addition of monomeric units to a growing aggregate occurs; or (3) nucleation-dependent aggregation, characterized by the relatively slow formation of nucleus and followed by rapid growth of the aggregate.

Dynamic light scattering (DLS[1]) is widely used to study the kinetics of protein aggregation (*14*, *28*−*34*). This method allows determining the size of particles formed in the process of protein aggregation. Besides, if the system contains particles varying markedly in size, it is possible to obtain the characteristics of the particles of each type.

The purpose of the present work was to study the kinetics of thermal aggregation of β_L-crystallin at various protein concentrations by DLS. The effect of α-crystallin on the kinetics of thermal aggregation of β_L-crystallin was studied. The sizes of the aggregates formed during the thermal aggregation of β_L-crystallin in the absence or in the presence of α-crystallin were determined. On the basis of obtained results new ideas on the mechanism of protein aggregation and mechanisms of the chaperone-like activity have been developed.

EXPERIMENTAL PROCEDURES

Isolation and Purification of Crystallins. Freshly excised lenses from 2-year-old steers were obtained from a local slaughterhouse and stored frozen at −20 °C. Purification of α- and β_L-crystallins was performed according to the procedure described earlier (*35*). The decapsulated lens cortex was homogenized at 0 °C in 40 mM sodium phosphate, pH 6.8, containing 100 mM NaCl, 1 mM EDTA, and 3 mM NaN_3. The homogenate was centrifuged at 27000*g* for 1 h at 4 °C, and the supernatant containing the soluble crystallins was fractionated by gel filtration using TSK-gel HW-55 (Sigma) column. The fraction containing α-crystallin was eluted in the void volume. The peak corresponding to β_L-crystallin was collected by measuring absorbance at 280 nm. Further purification of α- and β_L-crystallins was achieved by rechromatography of the crystallin-containing fractions using TSK-gel HW-55 and Sephacryl S200 (Sigma) columns, respectively. Finally, peaks corresponding to α- or β_L-crystallins were collected and concentrated by ultrafiltration (Millipore PTTK disk membrane (Sigma), NMWL 30,000). Crystallin concentrations were calculated using molar extinction coefficient of 0.85 $cm^2\ mg^{-1}$ for α-crystallin and 2.3 $cm^2\ mg^{-1}$ for β_L-crystallin (*21*).

Calorimetric Studies. Thermal denaturation of β_L-crystallin was studied by differential scanning calorimetry (DSC). DSC experiments were performed on a DASM-4M differential scanning microcalorimeter (Institute for Biological Instrumentation, Pushchino, Russia). All measurements were performed in 40 mM sodium phosphate, pH 6.8, containing 100 mM NaCl, 1 mM EDTA, and mM NaN_3. Protein solution (1.0−1.5 mg/mL) was heated with a constant rate of 1 K/min from 5 to 90 °C at the constant pressure of 2.2 atm. The reversibility of the thermal transitions of β_L-crystallin was tested by checking the reproducibility of the calorimetric trace in a second heating of the sample, which followed immediately after cooling. The thermal denaturation of β_L-crystallin was found to be fully irreversible. Calorimetric traces of β_L-crystallin were corrected for instrumental background and for possible aggregation artifacts by subtracting the scans obtained from the second heating of the samples. The temperature dependence of the excess heat capacity was further analyzed and plotted using Origin software (MicroCal Inc.).

DLS Studies. DLS is commonly used to determine the size of nanoparticles in a suspension by measuring the dynamics of the light-scattering intensity fluctuations (*36*). The diffusion coefficient D of the particles is directly related to the decay rate τ_c of the time-dependent correlation function for the light-scattering intensity fluctuations:

$$D = \frac{1}{2\tau_c k^2} \tag{1}$$

where k is the wavenumber of the scattered light, $k = (2\pi n/\lambda)\sin(\theta/2)$, n is the refractive index of the solvent, λ is the wavelength of the incident light in a vacuum, and θ is the scattering angle. The mean hydrodynamic radius of the particles, R, can then be calculated according to the Stokes−Einstein equation:

$$D = \frac{k_B T}{6\pi\eta R} \tag{2}$$

where k_B is Boltzmann's constant, T is the temperature, and η is the shear viscosity of the solvent.

It is important to note that DLS is correctly applicable for the sizing of non-interacting particles. If the particles are involved in an aggregation process, they certainly interact. However, this method can be successfully used to monitor the change in the apparent ("effective") particle size if the characteristic time of aggregation kinetics is much higher than the time of the measurements. The commercial DLS setup Photocor Complex is used (Photocor Instruments Inc., USA; www.photocor.com). Features of the Photocor Complex setup are typical in multipurpose installations for studying both static (intensity) and dynamic (time-dependent correlation function) light scattering *(37)*. A He−Ne laser (Coherent, model 31-2082, 632.8 nm, 10 mW) is used as a light source. The temperature of the sample cell is controlled by the PID temperature controller to within ±0.1 °C. To improve accuracy of measurement of small particles, a quasi-cross correlation photon counting system with two PMTs is used. This system allows measuring the particle size in a very wide range of 1 nm to 5 μm. The correlation function of light scattering fluctuations is analyzed by a single-board

[1] Abbreviations: DLS, dynamic light scattering; DSC, differential scanning calorimetry.

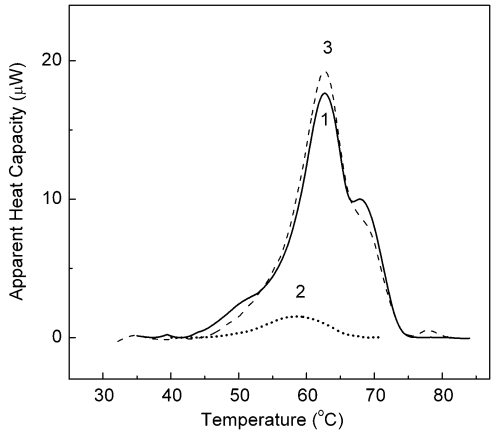

FIGURE 1: DSC profiles for isolated β_L-crystallin (1.5 mg/mL) (curve 1), isolated α-crystallin (1.2 mg/mL) (curve 2), and their mixture (curve 3). The conditions of the experiments: 40 mM Na-phosphate buffer, pH 6.8, 100 mM NaCl, 1 mM EDTA, and 3 mM NaN_3. The heating rate was 1 K/min.

correlator Photocor-FC, which has two time-scale modes of operation, namely, a linear mode with equidistant points of the measured correlation function and the so-called multiple-tau mode with the logarithmic order of the correlation points in time. Operation of the correlator in multiple-tau mode needs no tuning of time-scale and is suitable for measurements of multipeak particle distributions as well as for the sizing of growing particles in the course of aggregation. The linear scale of the correlator enables one to achieve the maximum accuracy for measurements of a monomodal narrow distribution. A personal computer was used to perform data analysis and instrument control. Polydispersity analysis was performed using DynaLS software (Alango, Israel). The kinetics of thermal aggregation of β_L-crystallin were studied by DLS in 40 mM sodium phosphate, pH 6.8, containing 100 mM NaCl, 1 mM EDTA, and 3 mM NaN_3, at 60 °C. All solutions for DLS experiments were prepared using deionized water obtained with Easy-Pure II RF system (Barnstead). The buffer was placed in a cylindrical cell with a diameter of 6.3 mm and preincubated for 10 min at 60 °C. Cells with stoppers were used for incubation at high temperature to avoid evaporation. The aggregation process was initiated by the addition of an aliquot of β_L-crystallin to a final volume of 0.5 mL. To study the effect of α-crystallin on aggregation of β_L-crystallin, aliquots of both crystallins were added into the cell simultaneously. When studying the kinetics of aggregation of β_L-crystallin, the scattering light was collected at 90° scattering angle.

Calculations. Origin 7.0 software (OriginLab Corporation) was used for calculations and construction of 3D plots.

RESULTS

Thermal Denaturation of β_L-Crystallin in the Absence or in the Presence of α-Crystallin. The heat sorption curve for isolated β_L-crystallin was represented by the main thermal transition at 62.5 °C with a small shoulder at ~68 °C (curve 1 in Figure 1). Isolated α-crystallin demonstrated a small thermal transition with a maximum at 59 °C (curve 2 in Figure 1). When the mixture of β_L-crystallin and α-crystallin was subjected to DSC analysis, the thermal transition of β_L-crystallin remained at the same position (62.5 °C) (curve 3 in Figure 1). The DSC results show that addition of α-crystallin has no appreciable influence on thermal denaturation of β_L-crystallin.

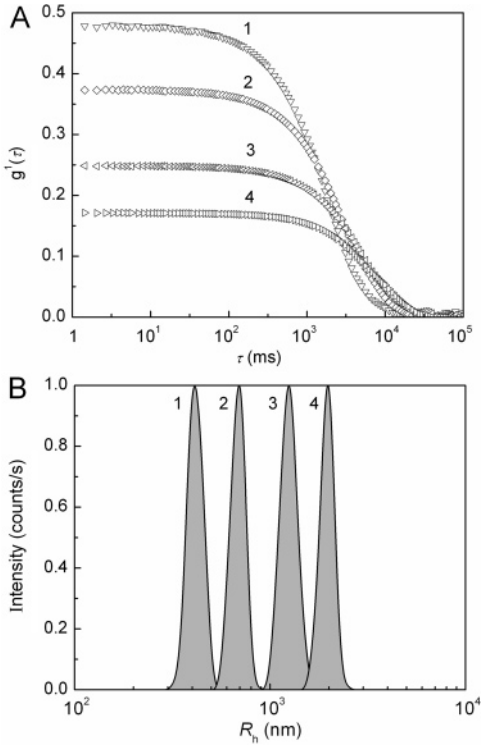

FIGURE 2: Thermal aggregation of β_L-crystallin (0.4 mg/mL) at 60 °C (40 mM Na-phosphate buffer, pH 6.8, containing 100 mM NaCl, 1 mM EDTA, and 3 mM NaN_3). Autocorrelation functions (A) and distributions of the particles with their size (B) registered at various times of incubation: 1, 15; 2, 20; 3, 30; and 4, 50 min.

The Kinetics of Thermal Aggregation of β_L-Crystallin. We have used DLS to characterize the size of particles formed in the course of thermal aggregation of β_L-crystallin. Figure 2A shows the typical autocorrelation functions measured at various times of incubation of β_L-crystallin (0.4 mg/mL) in 40 mM sodium phosphate buffer, pH 6.8, containing 100 mM NaCl, 1 mM EDTA, and 3 mM NaN_3, at 60 °C. The distribution of protein aggregates by their size calculated by DynaLS software is represented in Figure 2B. It is worth noting that the distribution function remains monomodal in the course of aggregation. Since DLS allows measuring the changes in the light scattering intensity (I) and hydrodynamic radius (R_h) value of the formed aggregates, the kinetics of β_L-crystallin aggregation may be characterized by a three-dimensional plot constructed in the coordinates: time; hydrodynamic radius; intensity of light scattering. Figure 3 shows the typical plot of such a kind obtained for aggregation of β_L-crystallin at a concentration of 0.4 mg/mL. When the time value is higher than 63 min, the diminishing of the light scattering intensity occurs (data not shown) because of precipitation of the large-sized aggregates. The projections of the kinetic curve on the *XY*, *XZ*, and *YZ* planes give, respectively, the R_h versus t, I versus t, and I versus R_h two-dimensional plots.

It is of special interest to analyze the character of the dependence of the light scattering intensity on the hydrodynamic radius. Such dependences are obtained at concentrations of β_L-crystallin varied in the interval from 0.025 to 0.4 mg/mL (Figure 4A). As can be seen from this figure, the dependences of I on R_h are linear (strictly speaking, they

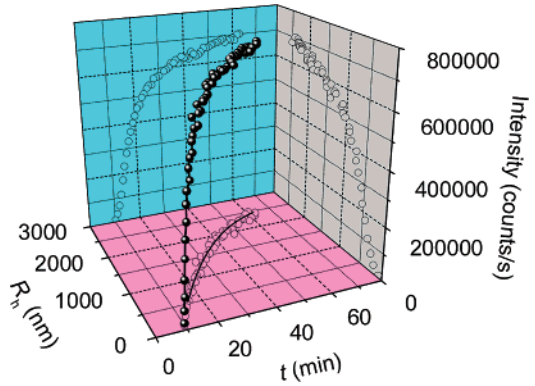

FIGURE 3: The 3D plot demonstrating the time course of the light scattering intensity and hydrodynamic radius (R_h) for thermal aggregation of β_L-crystallin (0.4 mg/mL) at 60 °C. *X* axis is time, *Y* axis is R_h, and *Z* axis is the light scattering intensity. The projections show the dependence of the R_h on time (*XY* projection), the dependence of the light scattering intensity on time (*XZ* projection), and the dependence of the light scattering intensity on R_h (*YZ* projection). Solid curve on *XY* projection is calculated from eq 4.

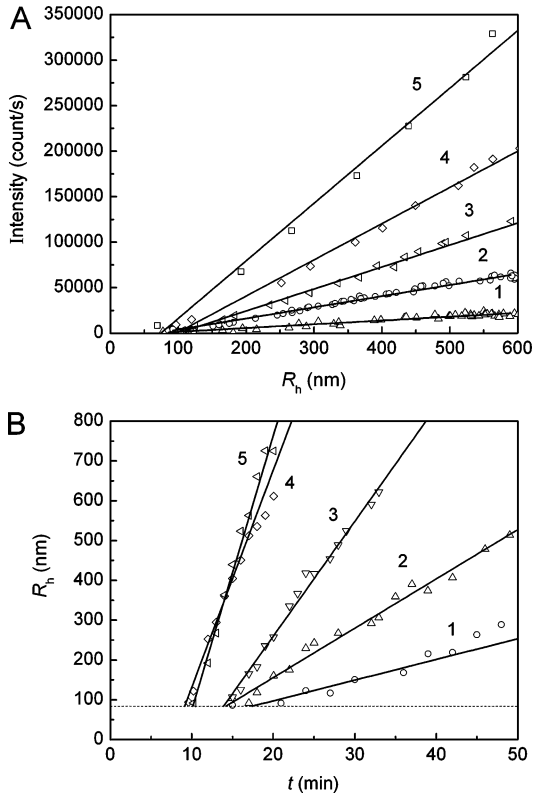

FIGURE 4: The characteristics of the latent stage for thermal aggregation of β_L-crystallin. The dependences of the light scattering intensity on the hydrodynamic radius (A) and the dependences of the hydrodynamic radius on time (B) obtained at various concentrations of β_L-crystallin: 1, 0.025; 2, 0.05; 3, 0.1; 4, 0.2; and 5, 0.4 mg/mL. The dotted line in panel B corresponds to the value of R_h for the start aggregates ($R_{h,0}$ = 84 nm).

are linear for the selected range of the R_h values). The length on the R_h axis cut off by the straight line corresponds to the size of the start aggregates detected at the instant of an initial increase in the light scattering intensity. The hydrodynamic radius of the start aggregates is denoted as $R_{h,0}$. All dependences of *I* on R_h obtained at various concentrations of β_L-crystallin cut off the same length on the abscissa axis (Figure 4A). This means that the $R_{h,0}$ value is independent

Table 1: The Effect of α-Crystallin on the Parameters of the Latent Stage for Thermal Aggregation of β_L-Crystallin (0.4 mg/mL) at 60 °C

concn of α-crystallin, mg/mL	t_{crit}, min	$R_{h,crit}$, nm	$R_{h,0}$, nm	t_0, min
0			81 ± 3	10.1 ± 0.1
0.025			31 ± 3	17.0 ± 0.3
0.05	25	250	31 ± 2	16.3 ± 0.3
0.1	65	250	25 ± 1	15.7 ± 0.5
0.15	80	35	21 ± 1	23 ± 3

of the β_L-crystallin concentration. The average value of $R_{h,0}$ is equal to 84 ± 4 nm. To determine the duration of the latent stage leading to the formation of the start aggregates, we used the R_h versus time plots (Figure 4B). First, we draw a horizontal line corresponding to the level $R_h = R_{h,0}$ (84 nm). In the interval of the selected values of time the dependences of R_h on time are linear. The length on the above-mentioned horizontal line cut off by the straight line in these coordinates corresponds to the duration of the latent stage (t_0). As can be seen from Figure 4B, the t_0 value increases from 10 to 16 min, when the concentration of β_L-crystallin decreases from 0.4 to 0.025 mg/mL.

To check the reversibility of thermal aggregation of β_L-crystallin the following experiments were performed. The β_L-crystallin solution (0.4 mg/mL, 40 mM sodium phosphate, pH 6.8, containing 100 mM NaCl, 1 mM EDTA, and 3 mM NaN_3) was heated at 60 °C for 20 min. The R_h value for the formed aggregates was 810 nm. The subsequent cooling of β_L-crystallin samples to 20 °C or 10-fold dilution by the same buffer did not result in the decrease in the aggregate size. Thus, thermal aggregation of β_L-crystallin proceeds irreversibly.

The Effect of α-Crystallin on the Kinetics of β_L-Crystallin Aggregation. Figure 5 shows the kinetics of β_L-crystallin (0.4 mg/mL) aggregation in the presence of α-crystallin. The concentration of α-crystallin was varied in the interval from 0.025 to 0.8 mg/mL. The higher was concentration of α-crystallin, the more marked was the suppression of the increment of the light scattering intensity in the course of aggregation (Figure 5A−E).

In the presence of α-crystallin protein aggregates demonstrate complicated dynamics of the R_h value change in time. At rather low concentration of α-crystallin (0.025 mg/mL; Figure 5F) the distribution of the protein aggregates by their size remains monomodal with time, and the R_h value increases slower than that for the control curve. At higher concentration of α-crystallin (0.05 mg/mL; Figure 5G) the distribution of the protein aggregates is monomodal ranging up to 25 min. When $t > 25$ min, two types of aggregates are registered. In addition to the basic aggregates (curve 1), the large-sized aggregates appear (curve 2). The point in time at which the size distribution function of the protein aggregates becomes bimodal is designated as t_{crit}. The R_h of the basic aggregates at $t = t_{crit}$ is denoted by $R_{h,crit}$. When the concentration of α-crystallin is equal to 0.05 mg/mL, $R_{h,crit} \approx 250$ nm. Bimodal distribution of protein aggregates by their size is also observed at concentrations of α-crystallin equal to 0.1 mg/mL (Figure 5H) and 0.15 mg/mL (Figure 5I). The increase in the α-crystallin concentration results in increasing the t_{crit} value ($t_{crit} \approx 65$ and 80 min at the α-crystallin concentration equal to 0.1 and 0.15 mg/mL,

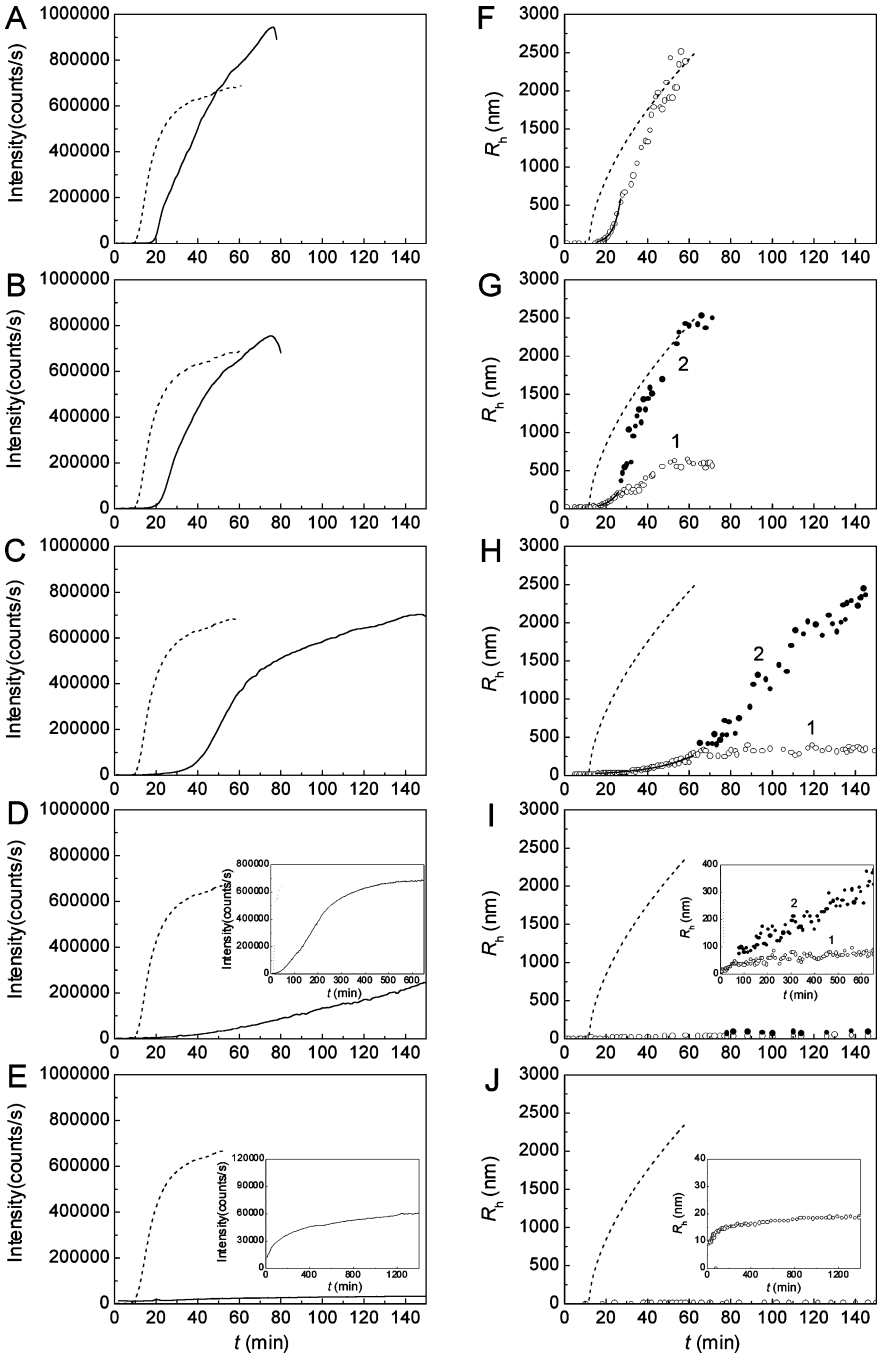

FIGURE 5: The effect of α-crystallin on the kinetics of thermal aggregation of β_L-crystallin (0.4 mg/mL) at 60 °C. The dependences of the intensity of light scattering (I) on time (panels A−E) and the dependences of the hydrodynamic radius (R_h) on time (panels F−J) obtained at various concentrations of α-crystallin: A and F, 0.025 mg/mL; B and G, 0.05 mg/mL; C and H, 0.1 mg/mL; D and I, 0.15 mg/mL; E and J, 0.8 mg/mL. The dotted lines in panels A−E correspond to the control (aggregation of β_L-crystallin in the absence of α-crystallin). Insets in panels D and E show the dependences of the light scattering intensity on time in a larger time interval. The dotted lines in panels F−J correspond to control (the dependence of R_h on time for aggregation of β_L-crystallin in the absence of α-crystallin). Insets in panels I and J show the dependences of R_h on t with the expanded ordinate axis. Curves 1 and 2 in panels G and H refer to the basic aggregates and superaggregates, respectively. The solid curves in panels F−I are drawn in accordance with eq 6.

respectively). The $R_{h,crit}$ values are found to be 250 and 35 nm, respectively (see Table 1). Superaggregates appear at $t > t_{crit}$. At higher concentration of α-crystallin (0.8 mg/mL) the aggregate population stops splitting into two components, and the hydrodynamic radius of the basic aggregates approaches the limiting value of 18.7 ± 0.1 nm during prolonged incubation (Figure 5J).

To characterize the influence of α-crystallin on the initial stage of β_L-crystallin aggregation, we have analyzed the initial parts of the kinetic curve of aggregation. The 3D plot in Figure 6 shows the initial part of the kinetic curve of β_L-crystallin (0.4 mg/mL) aggregation obtained at the concentration of α-crystallin equal to 0.1 mg/mL. The fact that the initial value of the light scattering intensity exceeds zero is connected with the presence of α-crystallin in the system. The DLS experiments were performed to determine the size of α-crystallin and its change in the course of heating at 60 °C. At the initial instant the R_h value for α-crystallin was found to be 9.6 ± 0.2 nm (40 mM sodium phosphate buffer, pH 6.8, containing 100 mM NaCl, 1 mM EDTA, and 3 mM

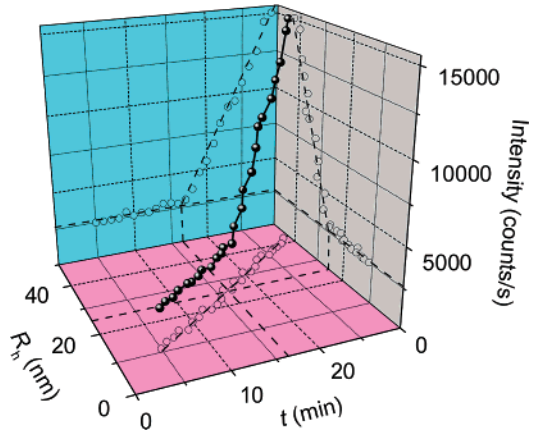

FIGURE 6: The 3D plot demonstrating the time course of the light scattering intensity and hydrodynamic radius (R_h) for thermal aggregation of β_L-crystallin (0.4 mg/mL) at 60 °C in the presence of α-crystallin (0.1 mg/mL). The dotted line on the *XY* projection corresponds to the value of R_h of the start aggregates ($R_{h,0}$ = 25 nm).

NaN_3). The R_h value varied slightly for 24 h incubation and run to 10.5 ± 0.2 nm. Thus, heating of α-crystallin under the defined conditions does not result in formation of large-sized aggregates.

The analysis of the dependence of light scattering intensity on the R_h value (the *XZ* projection in the 3D plot) for β_L-crystallin aggregation shows that the increase in the *I* value becomes marked at $R_h \geq 25$ nm. Thus, the hydrodynamic radius of the start aggregates is equal to 25 nm. As can be seen from the *XY* projection, the R_h value increases monotonically with time. The R_h value reaches the level $R_h = 25$ nm at $t = 15.7$ min. This value of time characterizes the duration of the latent stage ($t_0 = 15.7$ min). The break point in the dependence of the light scattering intensity on time (*XZ* projection) is also observed at $t = 15.7$ min.

The size of the start aggregates (the $R_{h,0}$ value) and duration of the latent stage (the t_0 value) for thermal aggregation of β_L-crystallin studied at various concentrations of α-crystallin are given in Table 1. The enhancement of the α-crystallin concentration results in the decrease in the $R_{h,0}$ value and simultaneous increase in the t_0 value.

DISCUSSION

Construction of the light scattering intensity versus the hydrodynamic radius plots has allowed us to conclude that the process of β_L-crystallin aggregation includes a latent stage. Over this stage the formation of aggregates is not detected by DLS because of their low concentration. The point in time at which the light scattering intensity is beginning to increase marks the completion of the latent stage and the onset of aggregation. We have designated the initial aggregates, whose size may be characterized quantitatively, as "the start aggregates". The hydrodynamic radius of the start aggregates ($R_{h,0}$) is estimated simply as a length on the R_h axis cut off by the linear dependence of the light scattering intensity on R_h.

We assume that formation of the start aggregate from isolated denatured molecules of β_L-crystallin is a process of cooperative association proceeding in accordance with the "all-or-none" principle. In other words, the concentration of intermediates (low-sized aggregates) is believed to be relatively small to be registered by DLS. The increment in the light scattering intensity registered in the aggregation experiments is predominantly due to sticking together of the start aggregates. For the diffusion-limited regime of aggregation, the dependence of the R_h on time obeys the power law (*38*):

$$R_h = R_{h,0}(1 + K_1 t)^{1/d_f} \quad (3)$$

where $R_{h,0}$ is the hydrodynamic radius of a seed particle, d_f is the fractal dimension, and K_1 is a constant. The fractal dimension is a structural characteristic of aggregates which are formed as a result of unordered interactions (random aggregation). The mass of an aggregate formed in such a way (*M*) is connected with its effective radius (*R*) by the following relationship: $M \sim R^{d_f}$. Since the process of aggregation of β_L-crystallin includes the nucleation stage, we used the modified form of eq 3 to demonstrate the validity of the power law for the dependence of R_h on time:

$$R_h = R_{h,0}\{1 + K_1(t - t_0)^{1/d_f}\} \quad (4)$$

where t_0 is the duration of lag period and *K* is a constant. As can be seen from Figure 3, the dependence of R_h on time for aggregation of β_L-crystallin (0.4 mg/mL) is described satisfactorily by eq 4 at $t > 15$ min. The following values of the parameters of eq 4 were obtained: $d_f = 1.78 \pm 0.06$, $K_1 = 0.2 \pm 1.6$ min^{-1}, and $t_0 = 13.3 \pm 0.4$ min.

For aggregation proceeding in the diffusion-limited regime a universal fractal dimension (d_f) of 1.8 is observed (*39*, *40*). Thus, one can assume that aggregation of β_L-crystallin registered by DLS is a process involving the interaction of the start aggregates. This process proceeds as a diffusion-limited aggregation. This means that each collision of the particles results in their sticking. To put it differently, sticking probability is equal to unity. It should be noted that if the growth of the aggregate proceeds by an attachment of the denatured protein molecule to the initial nucleus, the R_h would approach a limiting value at rather high values of time as the denatured protein is depleted (*27*).

Figure 5 demonstrates the preventing effect of α-crystallin on thermal aggregation of β_L-crystallin (0.4 mg/mL). The main result of the DLS study is that α-crystallin is incorporated in the growing aggregates at all concentrations used (0.025−0.8 mg/mL). Free α-crystallin is not found in the system. The decrease in the size of the start aggregates indicates that α-crystallin is incorporated in aggregates already at the nucleation stage. The start aggregates modified in this way stick together with a lesser rate. Deceleration of β_L-crystallin aggregation in the presence of α-crystallin is connected with the transition of the aggregation process from the regime of diffusion-limited aggregation to the regime of reaction-limited aggregation (the sticking probability becomes less than unity). If the reaction-limited regime is operative, the time course of the hydrodynamic radius obeys the exponential law (*40*):

$$R_h = R_{h,0} \exp(K_2 t) \quad (5)$$

where K_2 is a constant. If the aggregation process involves the nucleation stage, eq 5 is modified as follows:

$$R_h = R_{h,0} \exp[K_2(t - t_0)] \quad (6)$$

The initial parts of the dependences of R_h on time in the range of the time values from $t = t_0$ to $t = t_{crit}$ are described by eq 6 (solid curves in Figure 5F−I). When the concentration of α-crystallin is equal to 0.025 mg/mL, eq 6 is fulfilled in the time range from $t = t_0$ to 28 min. Parameter K_2 in eq 6 characterizes the rate of aggregation. The K_2 value decreases with increasing concentration of α-crystallin and is 0.283 ± 0.004 min^{-1} and 0.020 ± 0.001 min^{-1} at α-crystallin concentrations of 0.025 mg/mL and 0.15 mg/mL, respectively.

The appearance of two types of protein aggregates differing in size was registered by DLS in the case of thermal aggregation of bovine serum albumin at 58 °C (*34*) and aggregation of dithiothreitol-denatured α-lactalbumin (*30*). Krivandin et al. (*15*, *16*) observed the appearance of two types of aggregates at rather high times of incubation of the mixture of β_L-crystallin and α-crystallin at 60 °C.

To explain the splitting of the aggregate population into two components at $t > t_{crit}$, let us consider the nucleation stage. The start aggregates formed at the initial stage of the aggregation process have "sticky" regions participating in the interaction of the aggregating particles. We may call such sticky sites the "aggregation sites". Let us designate the start aggregates as A_1. The basic stage of the aggregation process is the interaction of particles A_i (a particle, containing i "monomers" A_1) and A_j (a particle, containing j "monomers" A_1):

$$A_i + A_j \rightarrow A_{i+j} \qquad (7)$$

This model of protein aggregation is identical to the model of the multimeric aggregation discussed by Speed et al. (*27*), provided that the "monomer" is the start aggregate A_1. Thus, the model we propose for thermal aggregation of β_L-crystallin involves the stage of formation of the start aggregate A_1 followed by aggregation of the multimers. It should be noted that aggregation of β_L-crystallin proceeds under the conditions where the denatured protein appears in the system. One can expect that the molecules of the denatured protein will add to the aggregates, thereby increasing the size of the latter.

Sticking together of the A_i and A_j particles results in the steric screening of part of the aggregation sites. In the absence of a chaperone the start aggregates with relatively high surface density of the sticking sites are formed, and screening of the part of the sticking sites in the interacting particles cannot prevent the formation of the large-sized aggregates prone to precipitation. However, incorporation of the chaperone into the start aggregates results in the reduction of the surface density of the aggregation sites. In this case, disappearance of the sticking sites in the aggregates formed as a result of their screening affects appreciably the character of the aggregation process. Interaction of the particles may bring about formation of aggregates in which all the sticking sites are saturated. The aggregates of such a type ("conservative aggregates") do not contain vacant sticking sites and are incapable of further growth. Formation of aggregates with completely saturated sticking sites may account for constancy of the R_h value for the small-sized aggregates under conditions of the splitting of the aggregate population into two components (Figure 5H and I). Apart from the conservative aggregates, the system always contains the population of aggregates, in which the aggregation sites are retained even at high values of time. The aggregates continue to stick together till the size values, at which precipitation occurs. Since aggregation of β_L-crystallin is an irreversible process, one can assume that interconversion between basic aggregates and superaggregates is lacking.

Our data show that at high concentrations of α-crystallin (i.e., under the conditions characteristic of mammal eye lens) only small-sized basic aggregates are formed. However, one can expect that decrease of the chaperone-like activity of α-crystallin as a result of posttranslational modifications (*5*, *9*, *10*) (this is similar to a decrease in concentration of the active α-crystallin) should bring about formation of the large-sized aggregates (superaggregates). The appearance of the large-sized aggregates may provoke the development of certain pathologies (particularly cataract).

The results of the study of the aggregation mechanism of β_L-crystallin and the mechanism of the chaperone-like activity of α-crystallin may be used in the screening of chemical agents, which block aggregation of β_L-crystallin and modulate the chaperone-like activity of α-crystallin.

REFERENCES

1. Horwitz, J. (1992) α-Crystallin can function as a molecular chaperone, *Proc. Natl. Acad. Sci. U.S.A. 89*, 10449−10453.
2. Augusteyn, A., and Stevens, A. (1998) Macromolecular structure of the eye lens, *Prog. Polym. Sci. 23*, 375−413.
3. Treweek, T. M., Morris, A. M., and Carver, J. A. (2003). Intracellular protein unfolding and aggregation: the role of small heat-shock chaperone proteins, *Aust. J. Chem. 56*, 357−367.
4. Delaye, M., and Tardieu, A. (1983) Short-range order of crystallin proteins accounts for eye lens transparency, *Nature 302*, 415−417.
5. Bloemendal, H. de Jong, W., Jaenicke, R. Lubsen, N. H., Slingsby, C., and Tardieu, A. (2004) Ageing and vision: structure, stability and function of lens crystallins, *Prog. Biophys. Mol. Biol. 86*, 407−485.
6. Boyle, D., and Takemoto, L. (1994) Characterization of the alpha-gamma and alpha-beta complex: evidence for an in vivo functional role of alpha-crystallin as a molecular chaperone, *Exp. Eye Res. 58*, 9−16.
7. Rao, P. V., Huang, Q. L., Horwitz, J., and Zigler, J. S., Jr. (1995) Evidence that alpha-crystallin prevents non-specific protein aggregation in the intact eye lens, *Biochim. Biophys. Acta 1245*, 439−447.
8. Horwitz, J. (2000) The function of alpha-crystallin in vision, *Semin. Cell Dev. Biol. 11*, 53−60.
9. Groenen, P. J., Merck, K. B., de Jong, W. W., and Bloemendal, H. (1994) Structure and modifications of the junior chaperone alpha-crystallin. From lens transparency to molecular pathology, *Eur. J. Biochem. 225*, 1−19.
10. Sun, Y., and MacRae, T. H. (2005) The small heat shock proteins and their role in human disease, *FEBS J. 272*, 2613−2627.
11. Wang, K., and Spector, A. (1994) The chaperone activity of bovine α-crystallin. Interaction with other lens crystallins in native and denatured states, *J. Biol. Chem. 269*, 13601−13608.
12. Raman, B., Ramakrishna, T., and Rao, C. M. (1995) Rapid refolding studies on the chaperone-like alpha-crystallin. Effect of alpha-crystallin on refolding of beta- and gamma-crystallins, *J. Biol. Chem. 270*, 19888−19921.
13. Saso, L., Grippa, E., Gatto, M. T., Leone, M. G., and Silvestrini, B. (2000) Inhibition of heat-induced aggregation of beta- and gamma-crystallin by alpha-crystallin evaluated by gel permeation HPLC, *Biochemistry (Moscow) 65*, 208−212.
14. Abgar, S., Vanhoudt, J., Aerts, T., and Clauwaert, J. (2001) Study of the chaperoning mechanism of bovine lens α-crystallin, a member of the a small heat shock superfamily, *Biophys. J. 80*, 1986−1995.
15. Krivandin, A. V., Muranov, K. O., and Ostrovsky, M. A. (2004) Heat-induced complex formation in solutions of alpha- and beta L-crystallins: a small-angle X-ray scattering study, *Dokl. Biochem. Biophys. (Moscow) 394*, 1−4.

16. Krivandin, A. V., Muranov, K. O., and Ostrovsky, M. A. (2004) Study of complexing between α- and β-crystallins in solutions at 60 °C, *Mol. Biol. (Moscow) 38*, 1−15.
17. Raman, B., and Rao, C. M. (1994) Chaperone-like activity and quaternary structure of alpha-crystallin, *J. Biol. Chem. 269*, 27264−27284.
18. Surewicz, W. K., and Olesen, P. R. (1995) On the thermal stability of alpha-crystallin: a new insight from infrared spectroscopy, *Biochemistry 34*, 9655−9660.
19. Das, B. K., Liang J. J., and Chakrabarti, B. (1997) Heat-induced conformational change and increased chaperone activity of lens alpha-crystallin, *Curr. Eye Res. 16*, 303−309.
20. Burgio, M. R., Kim, C. J., and Koretz, J. F. (2000). Characterization of the heat-induced quaternary transition of α-crystallin aggregates, *Invest. Ophthalmol. Visual Sci. 41*, S581.
21. Putilina, T., Skouri-Panet, F., Prat, K., Lubsen, N. H., and Tardieu, A. (2003) Subunit exchange demonstrates a differential chaperone activity of calf α-crystallin toward β_{LOW} -and individual γ-crystallins, *J. Biol. Chem. 278*, 13747−13756.
22. Regini, J. W., and Grossman, J. G. (2003) Structural changes of α-crystallin during heating and comparisons with other small heat shock proteins, *Fibre Diffr. Rev. 11*, 95−101.
23. Burgio, M. R., Kim, C. J., Dow, C. C., and Koretz, J. F. (2000) Correlation between the chaperone-like activity and aggregate size of alpha-crystallin with increasing temperature, *Biochem. Biophys. Res. Commun. 268*, 426−432.
24. MacRae, T. H. (2000) Structure and function of small heat shock: α-crystallin proteins: established concepts and emerging ideas, *Cell. Mol. Life Sci. 57*, 899−913.
25. Mandal, K., Dillon, J., and Gaillard, E. R. (2000) Heat and concentration effects on the small heat shock protein, α-crystallin, *Photochem. Photobiol. 71*, 470−475.
26. Devlin, J. G., Carver, L. A., and Bottomley, S. P. (2003) The selective inhibition of serpin aggregation by the molecular chaperone, α-crystallin, indicates a nucleation-dependent specificity, *J. Biol. Chem. 278*, 48644−48650.
27. Speed, M. A., King, J., and Wang, D. J. (1997) Polymerization mechanism of polypeptide chain aggregation, *Biotechnol. Bioeng. 54*, 333−343.
28. Andreasi, B. F., Arcovito, G., De Spirito, M., Mordente, A., and Martorana, G. E. (1995) Self-similarity properties of alpha-crystallin supramolecular aggregates, *Biophys. J. 69*, 2720−2727.
29. Sood, S. M. and Slattery, C. W. (2001) Association of mixtures of the two major forms of beta-casein from human milk, *J. Dairy Sci. 84*, 2163−2169.
30. Bettelheim, F. A., Ansari, R., Cheng, Q. F., and Zigler, J. S., Jr. (1999) The mode of chaperoning of dithiothreitol-denatured alpha-lactalbumin by alpha-crystallin, *Biochem. Biophys. Res. Commun., 261*, 292−297.
31. Modler, A. J., Gast, K., Lutsch, G., and Damaschun, G. (2003) Assembly of amyloid protofibrils via critical oligomers—a novel pathway of amyloid formation, *J. Mol. Biol. 325*, 135−148.
32. Baussay, K., Bon, L. C., Nicolai, T., Durand, D., and Busnel, J. P. (2004) Influence of the ionic strength on the heat-induced aggregation of the globular protein beta-lactoglobulin at pH 7, *Int. J. Biol. Macromol. 34*, 21−28.
33. Follmer, C., Pereira, F. V., DaSilveria, N. P., and Carlini, C. R. (2004) Jack bean urease (EC 3.5.1.5) aggregation monitored by dynamic and static light scattering, *Biophys. Chem. 111*, 79−87.
34. Militello, V., Casarino, C., Emanuele, A., Giostra, A., Pullara, F., and Leone, M. (2004) Aggregation kinetics of bovine serum albumin studied by FTIR spectroscopy and light scattering, *Biophys. Chem. 107*, 175−187.
35. Chiou, S. H., Azari, P., Himmel, M. E., and Squire, P. G. (1979). Isolation and physical characterization of bovine lens crystallins, *Int. J. Pept. Protein Res. 13*, 409−417.
36. *Photon Correlation and Light Beating Spectroscopy* (1974) (Cummins, H. Z., and Pike, E. R., Eds) Plenum, New York.
37. Yudin, I. K., Nikolaenko, G. L., Kosov, V. I., Agayan, V. A., Anisimov, M. A., and Sengers, J. V. (1997) Simple photon-correlation spectrometer for research and education, *Int. J. Thermophys. 18*, 1237−1248.
38. Lin, M. Y., Linsday, H. M., Weitz, D., A., Ball, R. C., Klein, R., and Meakin, P. (1989) Universality of fractal aggregates as probed by light scattering, *Proc. R. Soc. London, A 423*, 71−87.
39. Weitz, D. A., and Lin, M. Y. (1986) Dynamic scaling of cluster-mass distributions in kinetic colloid aggregation, *Phys. Rev. Lett. 57*, 2037−2040.
40. Weitz, D. A., Huang, J. S., Lin, M. Y., and Sung, J. (1985) Limits of the fractal dimension for irreversible kinetic aggregation of gold colloids, *Phys. Rev. Lett. 54*, 1416−1419.

BI051175U